ORNL/TM-6541

Pulse Pileup Effects on Plasma Electron Temperature Measurements by Soft X-Ray Energy Analysis

G. R. Dyer
G. H. Neilson
G. G. Kelley

OAK RIDGE NATIONAL LABORATORY
OPERATED BY UNION CARBIDE CORPORATION · FOR THE DEPARTMENT OF ENERGY

BLANK PAGE

ORNL/TM-6541
Dist. Category UC-20 f

Contract No. W-7405-eng-26

FUSION ENERGY DIVISION

PULSE PILEUP EFFECTS ON PLASMA ELECTRON TEMPERATURE MEASUREMENTS BY SOFT X-RAY ENERGY ANALYSIS

G. R. Dyer, G. H. Neilson, and G. G. Kelley

Date Published - October 1978

Prepared by the
OAK RIDGE NATIONAL LABORATORY
Oak Ridge, Tennessee 37830
operated by
UNION CARBIDE CORPORATION
for the
DEPARTMENT OF ENERGY

ABSTRACT

The electron temperature of hot plasmas is conveniently derived from bremsstrahlung spectra obtained by pulse-height analysis using a lithium-compensated silicon detector. Time-resolved temperature measurements require high counting rates, with ultimate rate limited by pulse pileup. To evaluate this limit, spectral distortion due to pileup and consequent effects on temperature determination are investigated. Expressions for distorted spectra are derived as functions of Maxwellian temperature and pileup fraction for both square and triangular pulse shapes. A comparison of temperatures obtained from distorted spectra with actual values indicates that measurements with less than 10% error can be made in the absence of line radiation, even from spectra containing 40% pileup.

A soft x-ray energy spectrometer using a single lithium-compensated silicon detector can be designed to operate at count rates in excess of 10^5/sec[1], but its successful application as a plasma diagnostic for time-resolved electron temperature measurements has been hampered by a lack of quantitative understanding of inherent systematic errors, chiefly spectral distortion due to pulse pileup. The energy analysis technique is not new to plasma diagnosis[2], but previous workers have avoided pulse pileup by sacrificing count rate capability, using multiple detectors, and incorporating pulse pileup rejection schemes in the spectrometer[3]. In a system optimized for the highest feasible count rate, some pulse pileup is inevitable, since effective pileup rejection depends on the availability of a counting channel which is fast compared with the data channel[4,5]. However, we show here that even if a bremsstrahlung spectrum from a Maxwellian plasma contains a considerable fraction of pileup pulses, the effect on temperature determination is small.

In an energy spectrometer, each detected photon results in an electrical pulse of fixed duration in time, with amplitude proportional to photon energy. Since shorter pulses introduce more white noise into the spectrometer signal channel, pulse duration cannot be made arbitrarily short; at present, 10^{-6} sec is the approximate limit for useful energy resolution. If a second photon is detected within the duration of a given pulse, a "piled-up" composite pulse results and is analyzed by the spectrometer and stored along with single-photon pulses, distorting the "true" energy spectrum. The pulse shape produced by a typical spectrometer amplifier is shown in fig. 1, along with square and

triangular pulse shapes of approximately the same duration. We analyze the expected spectral distortions using both the square pulse model (representing a "worst case" limit) and the triangular pulse model and determine the fraction of pileup pulses which may be tolerated in a spectrum.

The intensity distribution of photons from plasma bremsstrahlung radiation may be represented as[6)]

$$I(E) = \begin{cases} 0 , & E < E_0 \\ C' e^{-E/T_e} , & E \geq E_0 \end{cases} , \qquad (1)$$

where electron and ion density, ion charge, and electron temperature are assumed constant. The cutoff energy E_0 models the effect of the beryllium entrance window of the detector; typically $E_0 \approx 10^3$ eV. We introduce the normalized photon number distribution function, f(E), where

$$\int_{E_0}^{\infty} f(E)dE = 1 \qquad (2)$$

and

$$I(E) = N_0 E f(E) , \qquad (3)$$

where N_0 is the total number of photons in a spectrum. Thus, for brems-strahlung,

$$f(E) = \begin{cases} (C/E)e^{-E/T_e} , & E \geq E_0 \\ 0 , & E < E_0 \end{cases} , \qquad (4)$$

and $N_0 f(E)dE$ gives the number of photons in the energy range (E, E + dE).

Pulse pileup will distort the number distribution function of eq. (4). Assume that each detected photon of energy E produces a square pulse of height E and width τ, and let the mean time between pulses be T. Given a first pulse, a second pulse starting within the interval 2τ piles up on the first (see fig. 2). Both pulses are lost from their correct positions in the energy spectrum, and a single sum pulse is counted at energy

$$E_{sum} = E_1 + E_2 . \qquad (5)$$

The expected number of single and sum pulses in a measured spectrum may be derived by Poisson statistics[7]. The number of single pulses expected is

$$N_1 = N_0 e^{-2\tau/T} , \qquad (6)$$

and the number of two-pulse sums is

$$N_2 = 0.5\ N_0 (2\tau/T) e^{-2\tau/T} , \qquad (7)$$

where the factor 0.5 accounts for the two pulses in the sum. Note that N_1 and N_2 are independent of energy. If we define the pileup fraction K as

$$K = \tau/T \tag{8}$$

and stipulate that for our case $K \ll 1$, we can express eqs. (6) and (7) as expansions. To first order in K,

$$N_1 = N_0(1 - 2K) \tag{9}$$

and

$$N_2 = N_0K \ . \tag{10}$$

Note that in this approximation

$$N_1 + 2N_2 = N_0 \ ,$$

so for the condition $K \ll 1$, we neglect pileup events involving more than two photons.

An expression for the expected number of single-photon pulses having energy in (E, E + dE) can now be written as

$$dn_1(E) = N_1 f(E)dE \ . \tag{11}$$

The total energy of a two-photon sum pulse must satisfy eq. (5), so for component energies E_1 and E_2,

$$E_2 = E - E_1 \ . \tag{12}$$

For a fixed value of E_1, E_2 must be in $(E - E_1, E - E_1 + dE)$ in order to produce a sum pulse in (E, E + dE). The expected number of pileup

pulses $dn_2(E)$ with energies in (E, E + dE) is found by integrating over the possible combinations of constituent pulses:

$$dn_2(E) = N_2 dE \int_{E_0}^{E-E_0} f(E_1) f(E - E_1) dE_1 \ . \qquad (13)$$

Equation (13) is analytic for the form of f(E) given by eq. (4), so

$$dn_2(E) = \begin{cases} 2CN_2 f(E) dE \ \ln \dfrac{E - E_0}{E_0} & E > 2E_0 \\ 0 & E \leq 2E_0 \end{cases} . \qquad (14)$$

The total expected number of pulses dn(E) counted in (E, E + dE) can be obtained by combining eqs. (11) and (14):

$$dn(E) = dn_1(E) + dn_2(E)$$

or

$$dn(E) = \begin{cases} N_0 f(E) dE \left(1 - 2K + 2CK \ \ln \dfrac{E - E_0}{E_0}\right) & E > 2E_0 \\ N_0 f(E) dE \ (1 - 2K), & E \leq 2E_0 \end{cases} . \qquad (15)$$

If we define a distorted energy distribution function f'(E) which includes pileup effects so that

$$dn(E) = N_0 f'(E) dE \ ,$$

we can identify f'(E) from eq. (15).

$$f'(E) = \begin{cases} f(E)\left(1 - 2K + 2CK \ln \dfrac{E - E_0}{E_0}\right) & E > 2E_0 \\ f(E)(1 - 2K), & E \leqslant 2E_0 \end{cases} . \qquad (16)$$

From eqs. (3) and (4) we find that T_e is related to the bremsstrahlung intensity spectrum as

$$T_e = -\left\{\frac{d[\ln I(E)]}{dE}\right\}^{-1} \qquad (17)$$

and is independent of energy since ln (I) vs E is linear. If we define the pileup-distorted intensity distribution function as

$$I'(E) = N_0 E f'(E) , \qquad (18)$$

we see from fig. 3 that ln (I′) vs E is approximately linear for higher values of E. While a discussion of the optimum method for deriving a temperature from experimentally determined intensity vs energy data is beyond the scope of this paper, the general behavior of $(T_e)_d$, the derived temperature including pileup effects, can be found as follows. Select minimum and maximum energy limits for ln (I′) data, and fit a straight line to the ln (I′) vs E curve by the standard least-squares method. The negative inverse of the slope of this line is taken as $(T_e)_d$, which is a function of the energy limits selected and of the pileup fraction K. For the plots of $(T_e)_d$ given in fig. 3, the upper energy limit is fixed at 8 keV and $(T_e)_d$ is plotted as a function of the minimum energy limit for various values of K.

From fig. 3a, $(T_e)_d$ stays within 14% of T_e (=500 eV) even for K = 0.4, if the minimum energy limit is kept above 2.5 keV. Below 2.5 keV, the plots of ℓn (I′) vs E become sharply nonlinear, so this part of the spectrum should not be used in temperature derivations, according to the square-pulse model. At a temperature of 1 keV, the nonlinearity in ℓn (I′) extends to higher energies, but for a minimum energy limit of 3 keV or above, $(T_e)_d$ is still within 22% of T_e at K = 0.4.

The foregoing treatment based on a square pulse gives worst-case results, since any overlap at all between pulses results in the maximum sum amplitude. A more realistic analysis may be performed by using the symmetrical triangular pulse sketched in fig. 1; this pulse shape represents a good compromise between physical realism and analytic simplicity.

A review of the pulse-height analysis process for the triangular pulse aids in understanding the pileup distortion introduced by this model. The pulse-height analyzer examines each input pulse for a positive-to-negative slope transition; the first such transition in a pulse is identified as the peak, and subsequent transitions are ignored until the analyzer input falls below a preset baseline level. Thus, if pulse peaks are separated by time $t > \tau$, each pulse is properly analyzed and stored. For peak separation in the interval $\tau/2 < t < \tau$, the first pulse is properly analyzed but the second pulse is lost. For peak separations $t < \tau/2$, the analyzer registers a piled-up pulse.

Since the effect of pulse pileup is to remove some single pulses from their true place in a spectrum and to insert sum pulses where they do not belong, we define a number distribution function f′(E) which includes pileup effects:

$$f'(E) = f(E) - f_{\ell}(E) + f_{g}(E) \ , \tag{19}$$

where $f(E)$ is the undistorted function of eq. (4), $f_{\ell}(E)$ accounts for losses from the true spectrum, and $f_{g}(E)$ is the sum-pulse gain term. As in the square-pulse analysis, we consider only two-photon pileup.

To evaluate the loss term, we consider the probability that a given pulse of energy E is counted at some other energy, or is lost from the spectrum entirely. Referring to fig. 4, we note that a previous pulse starting within the time interval (a) with respect to the given pulse will cause the given pulse to be ignored by the analyzer, since the baseline will not be reached between pulses. The probability that a previous pulse will start within interval (a) is

$$P_{a} \approx \tau/2T \equiv 0.5K \ . \tag{20}$$

A previous pulse starting within interval (b) will combine with the given pulse to produce a sum pulse, and again the given pulse will not be counted correctly. The probability that this will happen is

$$P_{b} \approx \tau/T \equiv K \ . \tag{21}$$

A pulse may start anywhere outside intervals (a) and (b) without affecting the correct analysis of the given pulse. Thus, the counting loss at energy E due to pileup is given by

$$f_{\ell}(E) = f(E)(P_{a} + P_{b})$$

or

$$f_{\ell}(E) = \frac{3}{2} Kf(E) \quad . \tag{22}$$

Next consider the gain term. A sum pulse of amplitude E_s can be produced by a range of component pulses, depending on the degree of pulse overlap as well as component energy. Since all pulses have the same duration, the sum peak is always detected at the peak of the higher energy component; thus it is convenient to express the sum pulse energy as

$$E_s = E_h + \alpha E_{\ell} \quad , \tag{23}$$

where α is the degree of overlap of the component pulses and E_h and E_{ℓ} are the energies of the greater and smaller constituent pulses, respectively. It is obvious that E_h can be no smaller than E_0 or $E_s/2$, whichever is greater, so the following relations hold:

$$\left.\begin{matrix} E_s/2 \\ E_0 \end{matrix}\right] < E_h < E_s \tag{24}$$

and

$$\left.\begin{matrix} E_s - E_h \\ E_0 \end{matrix}\right] < E_{\ell} < E_h \quad . \tag{25}$$

We expect that the gain term will contain a double integral, since the higher energy pulse can range from $E_s/2$ to E_s in amplitude and each value of E_h can sum with a range of amplitudes E_{ℓ}, depending on the value of α. Figure 5 details the relations between the sum pulse and its components.

We wish to find the distribution function for E_s, the probability that components with energies E_h and E_ℓ sum to E_s within dE. From eq. (23)

$$\alpha E_\ell = E_s - E_h \ , \tag{26}$$

and from fig. 5,

$$\alpha = 2t/\tau \tag{27}$$

and

$$\alpha \delta E_\ell = dE \ . \tag{28}$$

Therefore, the probability that a pulse E_ℓ occurs in the interval (t, t + dt) with respect to the peak of the higher pulse and has the correct amplitude to sum with E_h to produce a pulse in the interval (E_s, E_s + dE) is

$$P_1 = f(E_\ell)\delta E_\ell \frac{dt}{T}$$

or

$$P_1 = (\tau/2t)f(E_\ell) \frac{dt}{T} dE \ . \tag{29}$$

From fig. 5,

$$t = \frac{\tau}{2} \cdot \frac{E_s - E_h}{E_\ell} \ , \tag{30}$$

so

$$\left|\frac{dt}{t}\right| = \left|\frac{dE_\ell}{E_\ell}\right| \ . \tag{31}$$

Thus,

$$P_1 = \frac{K}{2}\, dE f(E_\ell)\, \frac{dE_\ell}{E_\ell} \quad . \tag{32}$$

The probability P_2 that any pulse within the range of E_ℓ will pile up with E_h to produce a sum pulse in the interval $(E_s,\ E_s + dE)$ is found by integrating P_1 over the range of E_ℓ:

$$P_2 = \frac{K}{2}\, dE \int_{E_s - E_h}^{E_h} f(E_\ell)\, \frac{dE_\ell}{E_\ell} \quad . \tag{33}$$

Finally, the total probability P_s that two pulses will sum to E_s within dE is

$$P_s = f_g(E_s)dE = 2 \int_{E_s/2}^{E_s} P_2 f(E_h) dE_h \tag{34}$$

or

$$f_g(E_s) = K \int_{E_s/2}^{E_s} f(E_h) dE_h \int_{E_s - E_h}^{E_h} f(E_\ell)\, \frac{dE_\ell}{E_\ell} \quad . \tag{35}$$

The factor of two is inserted in eq. (34) because the lower energy pulse can sum on either its leading or trailing edge to produce E_s.

By inserting eqs. (22) and (35) into eq. (19), we arrive at the distribution function including pileup effects:

$$f'(E) = f(E)\left(1 - \frac{3}{2}K\right) + K\int_{E_s/2}^{E_s} f(E_h)dE_h \int_{E_s - E_h}^{E_h} f(E_\ell)\,\frac{dE_\ell}{E_\ell} \quad . \tag{36}$$

By substituting eq. (4) in eq. (36) and using the definition for I'(E) given in eq. (18), we can evaluate the effect of pileup on intensity as predicted by the triangular pulse model. $(T_e)_d$ is evaluated by the same least-squares fit to the ℓn (I') data as was used previously. Plots of ℓn (I') and $(T_e)_d$ vs E are given in fig. 6. Note that spectral distortion is not as severe for this case as for the square-pulse model, though the curves for ℓn (I') vs E still become decidedly nonlinear at approximately the same energies as before. For a minimum energy of 2.5 keV and T_e = 500 eV, $(T_e)_d$ is within 5% of T_e even for K = 0.4. At T_e = 1 keV and a minimum energy limit of 3 keV, $(T_e)_d$ is within 8% of T_e for K = 0.4.

Since the linear amplifier pulse shape of fig. 1 is approximated more closely by the triangular than by the square pulse, we expect that the actual distortion of a bremsstrahlung spectrum by pileup will be more accurately predicted by fig. 6, though both models are in qualitative agreement: pileup does cause spectral distortion and should be minimized or avoided where possible. However, even if experimental data do contain as much as 20-40% pileup pulses, it is still possible to derive electron temperature to within 10% of the true value from the distorted data without applying corrective procedures, provided the grossly nonlinear low energy region of the ℓn (I') spectrum is not used in the $(T_e)_d$ calculation. Furthermore, because the curves of ℓn (I') vs E behave in a predictable manner with increasing pileup, and because pileup fraction is estimable from total count rate measurements and amplifier pulse

shaping parameters, some degree of correction of experimental data for pileup effects is possible. The similarity of the square and triangular pulse analytical conclusions suggests that small differences between real and assumed amplifier pulse shapes are not important. These results indicate that data from a single-detector spectrometer optimized for high-count-rate operation can be used even when the most desirable data collection rate is exceeded, so the effective dynamic range of the diagnostic is extended. The analysis assumes that detected radiation is bremsstrahlung from a Maxwellian plasma; where experimental conditions approximate this premise, good temperature derivations by x-ray analysis are possible even in the presence of considerable pulse pileup.

REFERENCES

[1] *Fusion Energy Division Annual Progress Report for 1976*, ORNL-5275 (Oak Ridge National Laboratory, 1977), pp. 78-81.

[2] S. von Goeler et al., Nucl. Fusion 15 (1975) 301.

[3] S. von Goeler et al., *Soft X-Ray Measurements on the PLT Tokamak*, PPPL-1383 (Princeton Plasma Physics Laboratory, 1977).

[4] S. Rozen, Nucl. Instrum. Methods 11 (1961) 316.

[5] R. L. Heath and L. O. Johnson, IEEE-TNS 16, No. 5 (1969) 58.

[6] W. Lochte-Holtgreven, ed., *Plasma Diagnostics* (North Holland Publishing Company, Amsterdam, 1968), pp. 40-41.

[7] A. C. Melissinos, *Experiments in Modern Physics* (Academic Press, New York, 1966), pp. 438-453.

FIGURE CAPTIONS

Fig. 1. Typical amplifier pulse shape, with square and triangular pulses of similar duration.

Fig. 2. Square pulse and associated time interval during which pileup occurs.

Fig. 3a. $(T_e)_d$ vs E for T_e = 500 eV (square pulse model).

Fig. 3b. $\ell n(I')$ vs E for T_e = 500 eV (square pulse model).

Fig. 3c. $(T_e)_d$ vs E for T_e = 1 keV (square pulse model).

Fig. 3d. $\ell n(I')$ vs E for T_e = 1 keV (square pulse model).

Fig. 4. Triangular pulse and time intervals during which loss and pileup occur.

Fig. 5. Sum pulse and components.

Fig. 6a. $(T_e)_d$ vs E for T_e = 500 eV (triangular pulse model).

Fig. 6b. ℓn (I') vs E for T_e = 500 eV (triangular pulse model).

Fig. 6c. $(T_e)_d$ vs E for T_e = 1 keV (triangular pulse model)

Fig. 6d. ℓn (I') vs E for T_e = 1 keV (triangular pulse model).

ORNL/DWG/FED 78-805

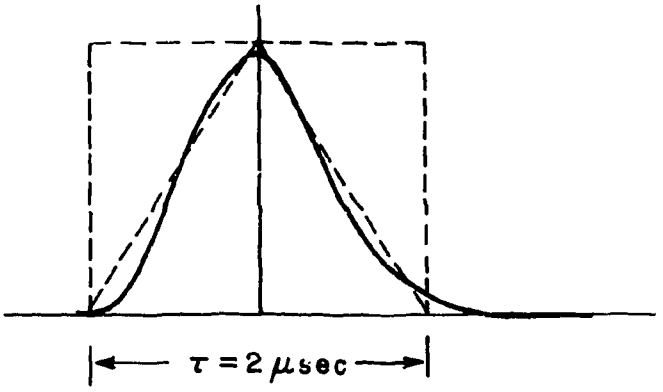

Fig. 1.

ORNL/DWG/FED 78-806

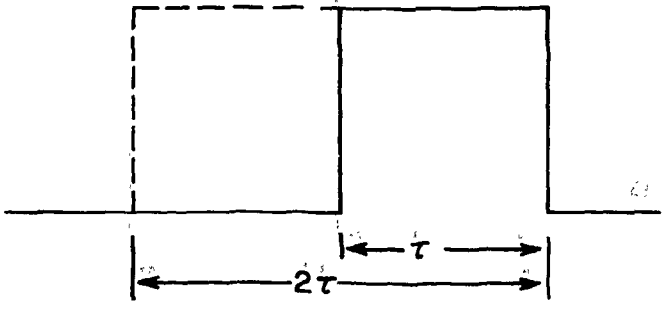

Fig. 2.

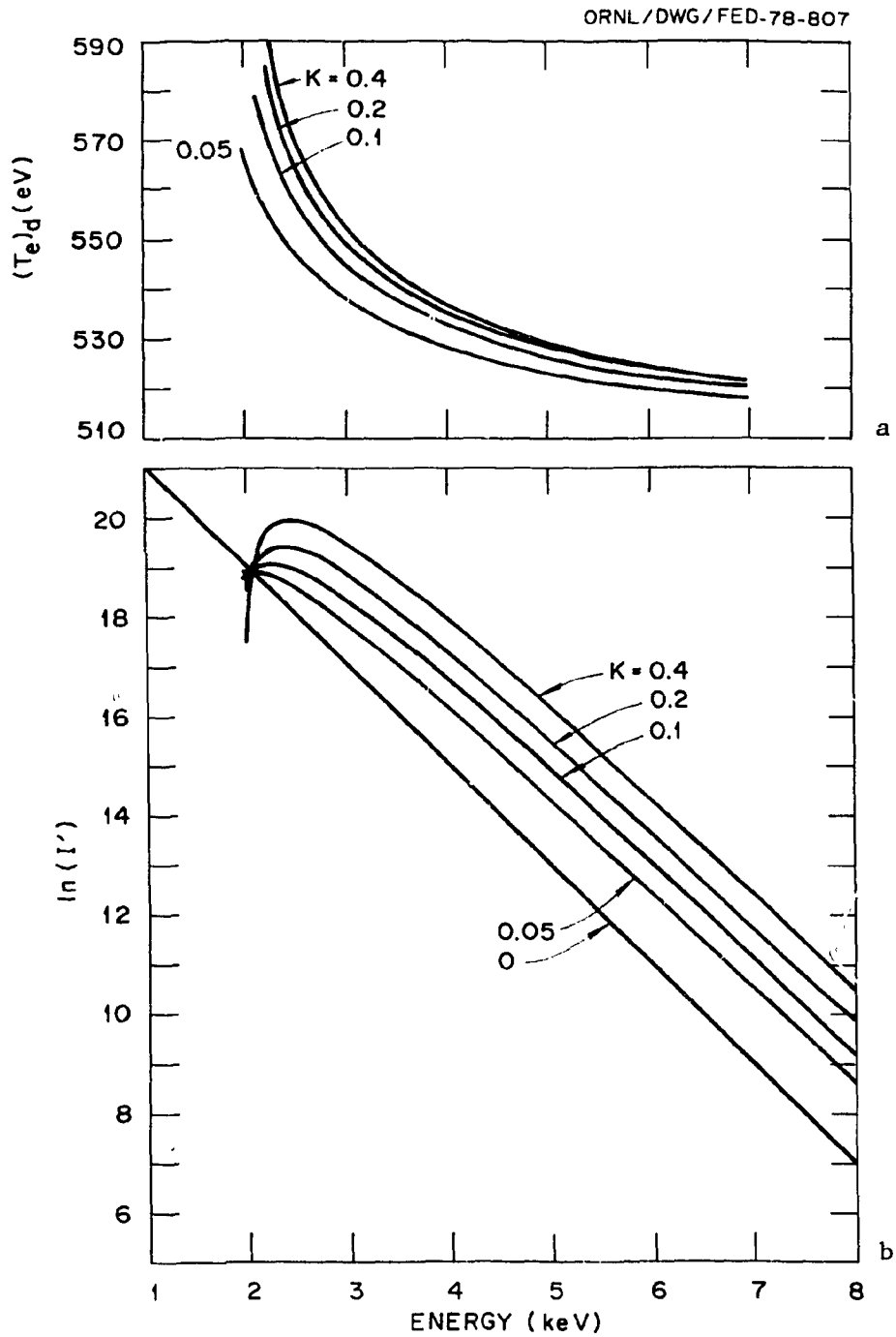
ORNL/DWG/FED-78-807
590
570
550
530
510
$(T_e)_d$(eV)
K = 0.4
0.2
0.1
0.05
a
20
18
16
14
12
10
8
6
ln(I')
K = 0.4
0.2
0.1
0.05
0
b
1
2
3
4
5
6
7
8
ENERGY (keV)

Fig. 3.

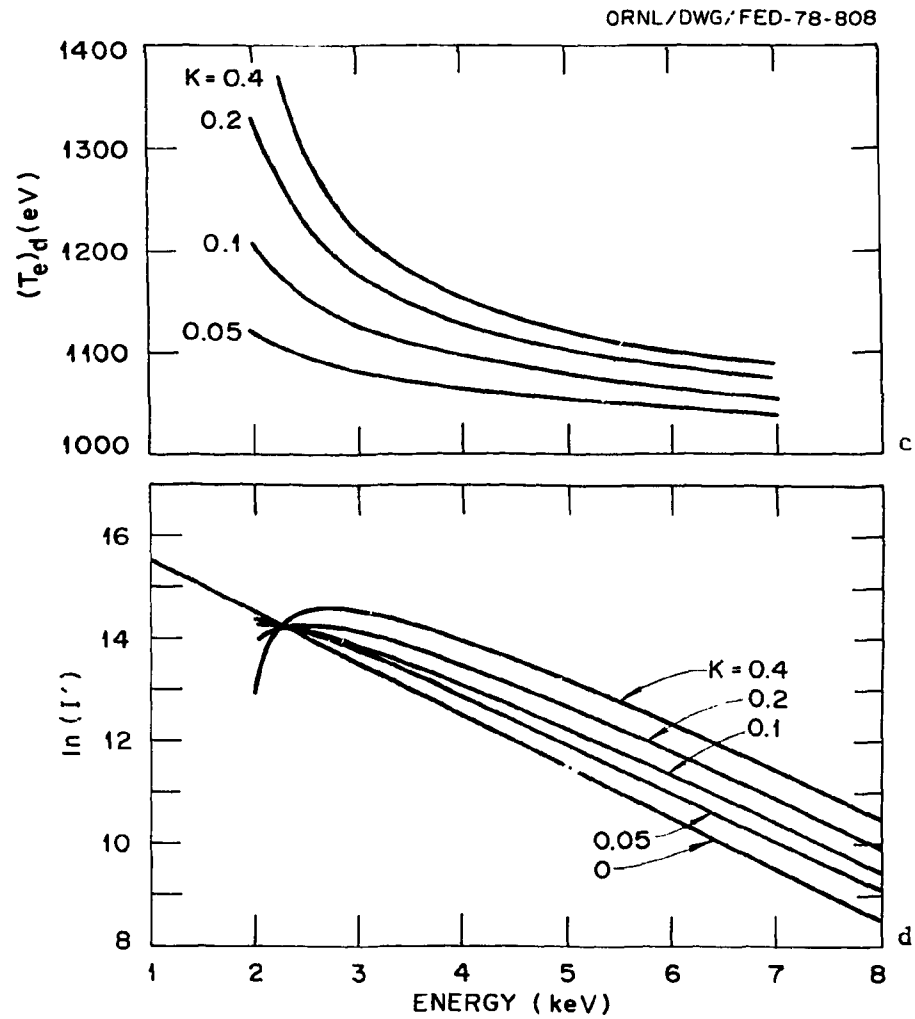
ORNL/DWG/FED-78-808
1400
1300
1200
1100
1000
$(T_e)_d$ (eV)
K = 0.4
0.2
0.1
0.05
c
16
14
12
10
8
ln (I')
K = 0.4
0.2
0.1
0.05
0
d
1
2
3
4
5
6
7
8
ENERGY (keV)

Fig. 3.

ORNL/DWG/FED 78-809

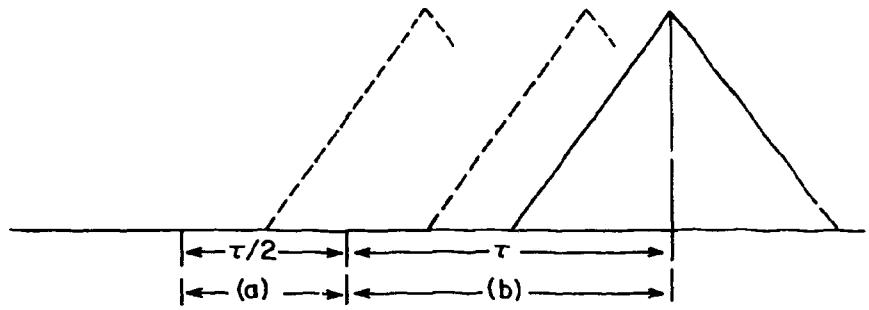

Fig. 4.

ORNL/DWG/FED 78-810

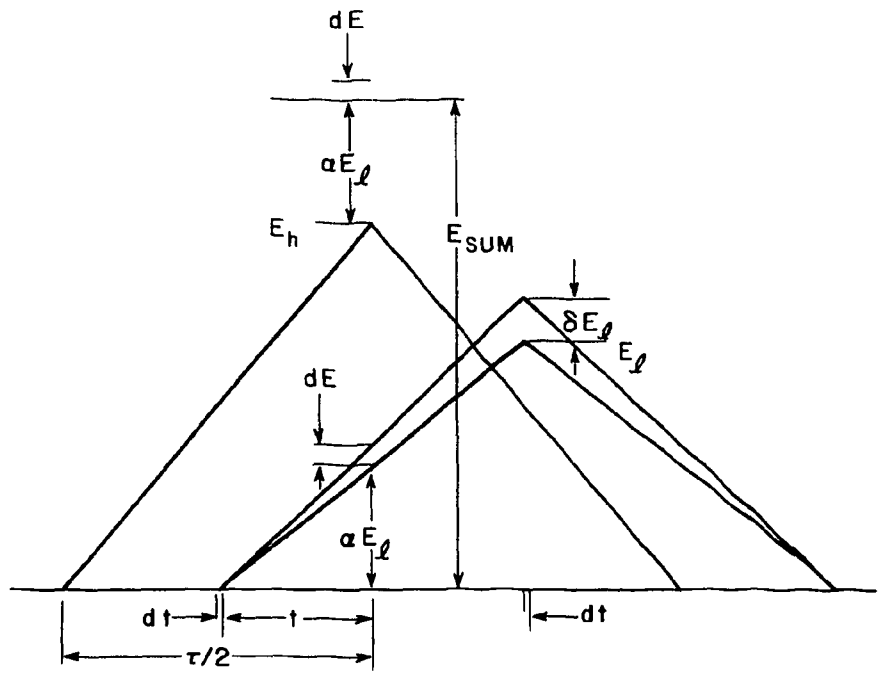

$\alpha = 2t/\tau$

$dE = \alpha \delta E_\ell$

$t = (\tau/2)\ \dfrac{E_{SUM} - E_h}{E_\ell}$

$t_{MAX} = \tau/2$

$t_{MIN} = (\tau/2)\ \dfrac{E_{SUM} - E_h}{E_h}$

$(E_\ell)_{MIN} = E_{SUM} - E_h$

$\alpha = 1$ for $(E_\ell)_{MIN}$

$(E_\ell)_{MAX} = E_h$

$\alpha = \dfrac{E_{SUM} - E_h}{E_h}$ for $(E_\ell)_{MAX}$

Fig. 5.

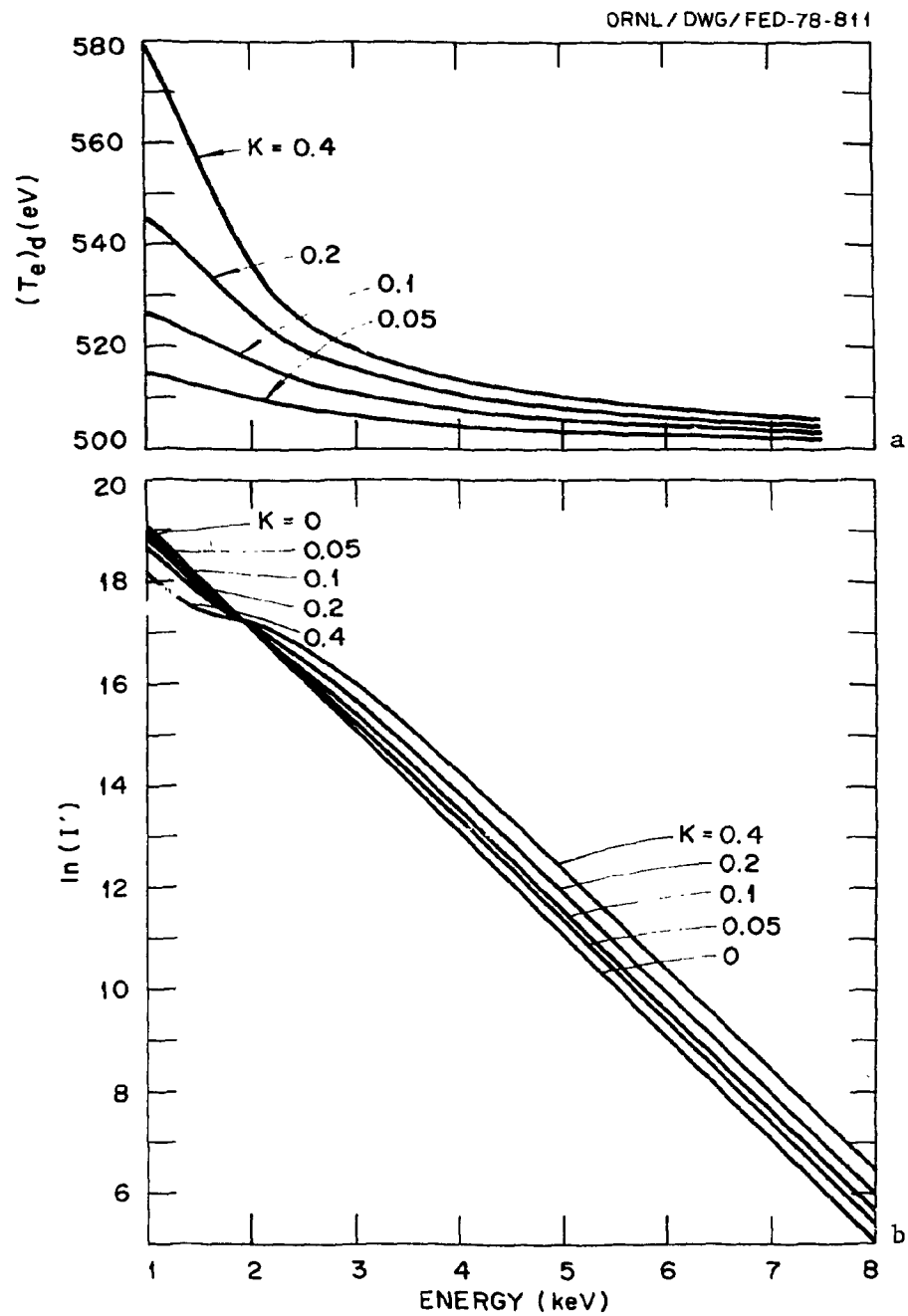
ORNL / DWG / FED-78-811
580
560
540
520
500
$(T_e)_d$ (eV)
K = 0.4
0.2
0.1
0.05
a
20
18
16
14
12
10
8
6
ln (I')
K = 0
0.05
0.1
0.2
0.4
K = 0.4
0.2
0.1
0.05
0
b
1
2
3
4
5
6
7
8
ENERGY (keV)

Fig. 6.

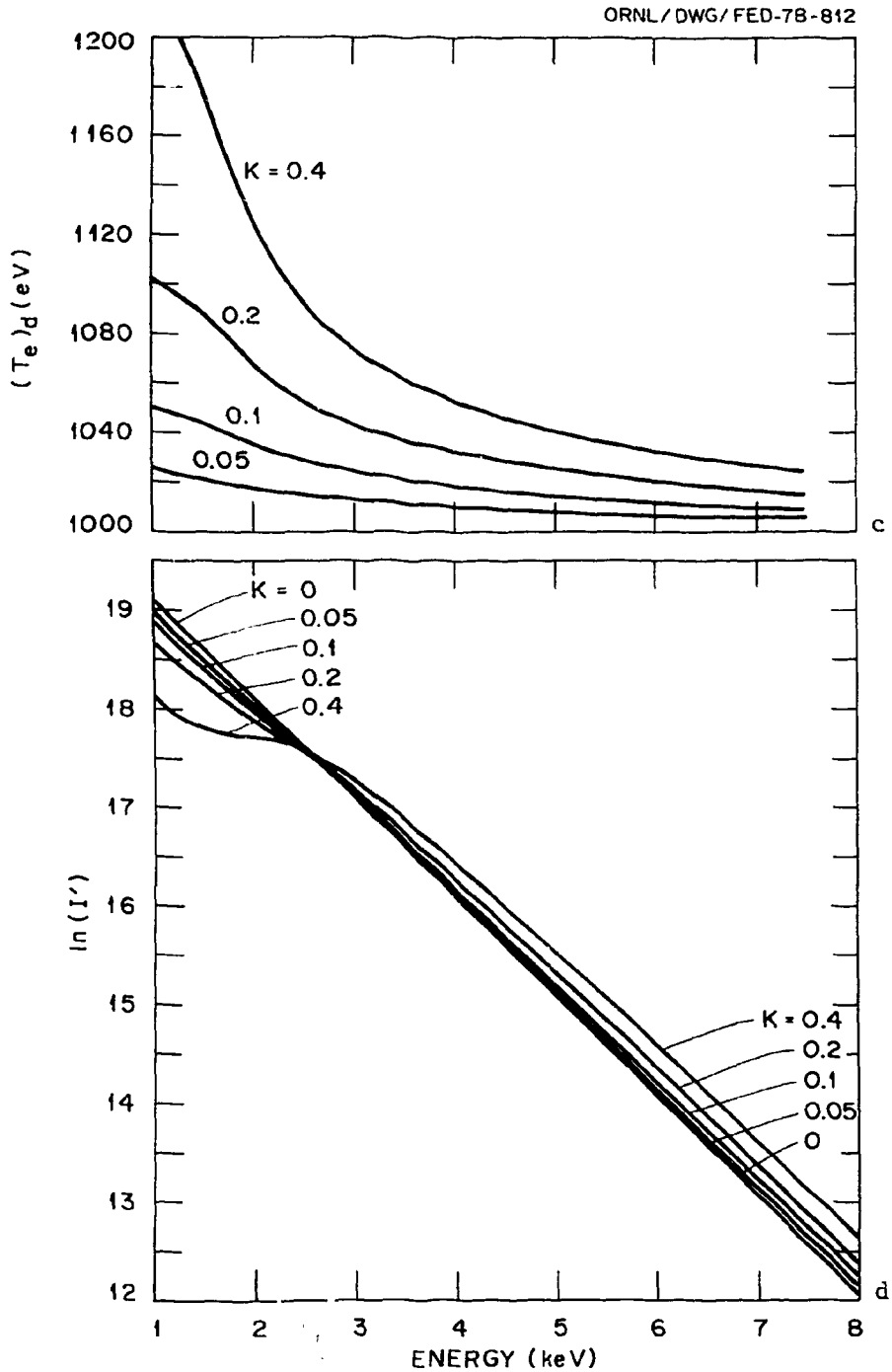
ORNL/DWG/FED-78-812
1200
1160
1120
1080
1040
1000
$(T_e)_d$ (eV)
K = 0.4
0.2
0.1
0.05
c
K = 0
0.05
0.1
0.2
0.4
19
18
17
16
15
14
13
12
ln (I')
K = 0.4
0.2
0.1
0.05
0
d
1
2
3
4
5
6
7
8
ENERGY (keV)

Fig. 6.

ORNL/TM-6541
Dist. Category UC-20 f

INTERNAL DISTRIBUTION

1. S. C. Bates
2. C. F. Barnett
3. R. L. Becker
4. L. A. Berry
5. J. D. Callen
6. J. L. Dunlap
7-50. G. R. Dyer
51. P. H. Edmonds
52. O. C. Eldridge
53. G. R. Haste
54. G. G. Kelley
55. E. J. Kennedy
56. J. F. Lyon
57. O. B. Morgan
58. M. Murakami
59. G. H. Neilson
60. D. R. Overbey
61. H. Postma
62. J. A. Ray
63. M. W. Rosenthal
64. M. J. Saltmarsh
65. J. Sheffield
66. D. W. Swain
67. J. B. Wilgen
68. W. R. Wing
69-70. Central Research Library
71. Document Reference Section
72. Fusion Energy Division Library
73. Fusion Energy Division Communications Center
74-75. Laboratory Records Department
76. Laboratory Records, ORNL-RC
77. ORNL Patent Office

EXTERNAL DISTRIBUTION

78. D. J. Anthony, Energy Systems and Technology Division, General Electric Company, 1 River Road, Bldg. 23, Room 290, Schenectady, NY 12345
79. Joel Ayers, ORTEC, Inc., Midland Road, Oak Ridge, TN 37830
80. P. R. Bell, 132 Westlook Circle, Oak Ridge, TN 37830
81. J. F. Clarke, Office of Fusion Energy, Department of Energy, Washington, DC 20545
82. N. A. Davies, Tokamak Branch, Office of Fusion Energy, Department of Energy, Washington, DC 20545
83. S. O. Dean, Office of Confinement Systems, Office of Fusion Energy, Department of Energy, Washington, DC 20545
84. H. K. Forsen, Exxon Nuclear Company, Inc., 777 106th Ave., N.E., Bellevue, WA 98009
85. H. P. Furth, Princeton Plasma Physics Laboratory, P.O. Box 451, Princeton, NJ 08540
86. D. A. Gedcke, ORTEC, Inc., Midland Road, Oak Ridge, TN 37830
87. R. W. Gould, California Institute of Technology, Mail Stop 116-81, Pasadena, CA 91125
88. C. C. Harris, Dept. of Nuclear Medicine, Duke University, Durham, NC 27706
89. E. G. Harris, Dept. of Physics, University of Tennessee, Knoxville, TN 37916

90. K. W. Hill, Princeton Plasma Physics Laboratory, P.O. Box 451, Princeton, NJ 08540
91. R. L. Hirsch, Exxon Research and Engineering Co., P.O. Box 101, Florham Park, NJ 07932
92. T. Hsu, Office of Confinement Systems, Office of Fusion Energy, Department of Energy, Washington, DC 20545
93. G. L. Jahns, General Atomic Co., P.O. Box 81608, San Diego, CA 92138
94. D. H. McNeill, Princeton Plasma Physics Laboratory, P.O. Box 451, Princeton, NJ 08540
95. John Rice, Francis Bitter National Magnet Laboratory, Massachusetts Institute of Technology, Cambridge, MA 02139
96. R. H. Rohrer, Dept. of Physics, Emory University, Atlanta, GA 30322
97. M. M. Satterfield, The Nucleus, 461 Laboratory Road, Oak Ridge, TN 37830
98. R. J. Taylor, Center for Plasma Physics and Fusion Engineering, University of California, Los Angeles, CA 90024
99. S. von Goeler, Princeton Plasma Physics Laboratory, P.O. Box 451, Princeton, NJ 08540
100. Director, Research and Technical Support Division, Department of Energy, Oak Ridge Operations, P.O. Box E, Oak Ridge, TN 37830

101-289. Given distribution as shown in TID-4500, Magnetic Fusion Energy (Distribution Category UC-20 f, Experimental Plasma Physics)